Transient Modeling of Z-Source Chopper with and without ESR used for Control of Capacitor Voltage

BYAMAKESH NAYAK[1], SASWATI SWAPNA DASH[2]
[1]Department of Electrical Engineering, [2]Department of Electrical Engineering
KIIT University[1], YMCA University of science and technology[2]
[1]Bhubaneswar,odisha [2]Faridabad,Haryana
INDIA
electricbkn@gmail.com[1], reachtoswapna@gmail.com[2]

Abstract: - The newly proposed Z-source chopper with two controlled switches is used to stabilize the duty cycle above 0.5 is presented. The device has boost capability without polarity reversal in the range of duty cycle 0 to 0.5 and buck-boost capability with polarity reversal of output voltage in the range of duty cycle 0.5 to 1. The above capabilities of the topology are studied through simulation. This paper also presents transient modeling of the proposed Z-source chopper with and without ESR (equivalent series resistance). The effects of ESR are studied in depth and based upon the transient modeling; the dc-link voltage is controlled by direct measurement of capacitor voltage and inductor current. The presence of RHP (right-half-plane) zero in developed average control-to-output model reveal that the output decreases initially before rising toward its new steady-state value when a step increase in control input is applied. The non-minimum-phase transient response can be reduced by proper feed-back control technique. Compensator for both voltage mode and current mode control are designed using classical control technique through small-signal-analysis. Hysteresis band modulator is used for finding out the switching function of switches. Performance of control method of the compensated Z-source chopper is verified by simulation.

Key-Words: - Z-source chopper, Current mode control (CMC), Hysteresis band modulator, Buck-Boost capabilities, Non–minimum–phase transient response, ESR (Equivalent series resistance), RHP (Right-half-plane).

1 Introduction

Nowadays there is a rapid development in the field of various applications of power electronics. The previous literatures on Z-source chopper uses only one controlled switch and other one is diode. With one controlled switch and one uncontrolled switch, the control range of duty cycle period is limited to 0.5, because of diode will remain on the entire period, if the duty cycle is above 0.5.Since the duty cycle period is limited to 0.5,the circuit can be only boost mode capability without polarity reversal. The previous literatures only deal with one controlled switch and diode with inductors and capacitors arranged in X shape to boost up the output voltage with polarity same as the input voltage using shoot through technique [1] and the performance analysis is done [2]. The duty cycle period of previous literature circuit is limited to 0.5, because of, above 0.5 the diode is forward biased and therefore it remains on for whole the period makes the circuit unstable. The unstable range of duty cycle period can be eliminated using controlled switch instead of diode so the output voltage can be controlled by controlling the duty period range from 0 to 1. This paper now presents the newly proposed Z-source chopper with battery as input that can be used for both buck and boost the input voltage. A simplified equivalent model of Z-source with R-L load is shown in Fig-1.

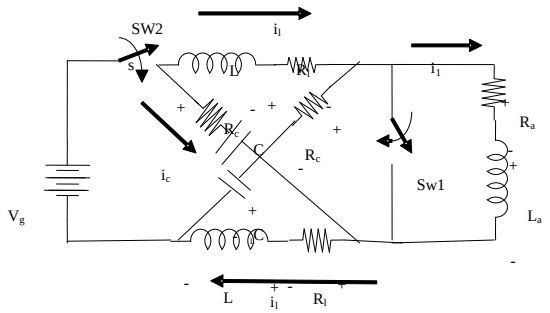

Fig 1: Circuit diagram of Z-source chopper with ESR of inductance and Capacitance

The newly proposed Z-source chopper is new single-stage electronics power converter utilizing impedance network with two controlled switches in such a way that voltage-boost capability without polarity reversal and boost-buck capability with polarity reversal are achieved by introducing shoot-through across the load. The above both voltage-buck and boost capability feature of Z- source

converter can be used in fuel energy conversion system and four quadrant speed control of dc motor drive system. The effect of parasitic component of inductor and capacitor are studied in detail. The battery-side phenomenon is associated with the value of inductance and capacitance in X shaped network, and is studied using small-signal analysis to show the presence of the right-half-plane (RHP) zero in the control-to-load current, control-to-inductor current and control-to-voltage transfer functions [3],[4]. Transient modeling of Z-source converter with R-L load is analyzed through state-space average analysis method to show its non-minimum-phase response caused by battery-side [5], [6], [7]. The passive parameters such as inductor and capacitor are selected based on ripple current and ripple voltage respectively by considering worst case condition. Dynamic modeling of Z-source with R-L load has been formulated using state-space averaged analysis method. Small signal model has been derived from the state-space averaged dynamic method for linearization. Based on small signal linearization model the control law for output voltage control is derived. Output voltage is controlled by direct measurement of the voltage and inductor current. The compensators for the voltage loop and the current loop are designed based on the frequency responses and as well as root locus technique. A hysteresis band modulator is used for improving transient response and tested in MATLAB/SIMULINK simulation using an efficient closed loop Z-source switching -functional model.

2 State-space Averaged Analysis of Z-source Chopper with R-L load

Operation of Z-source chopper with R-L load can be explained in two modes. Assuming continuous conduction mode, there are two modes one is called shoot through mode, where load is shorted by turning on the switch-1 and other is input connected mode where switch-1 is on to connect the input to load. As shown in Fig1, this converter has three energy storage elements so three state variables are needed to represent state-space model of Z-source chopper. The ESR (equivalent series resistance) of inductor and capacitor are taken into consideration for formulating state-space average model of Z-source chopper. The KVL, KCL expressions in terms of the inductor current, load current and capacitor voltage when switch-1 is on (switch-2 is off) are:

$$L\frac{di_l}{dt} + R_l i_l = v_c - R_c i_l \quad (1)$$

$$L_a\frac{di_1}{dt} + R_a i_1 = 0 \quad (2)$$

$$C\frac{dv_c}{dt} = i_c = -i_l \quad (3)$$

Where R_l and R_c represent ESR of inductance (L), ESR of capacitance(C) of X shaped network of chopper circuit. Ra and La is the load to z-source chopper.

The (1), (2) and (3) can be represented in state-space form as:

$\dot{X}=AX+BU$ and $Y=CX$

Where, $A = dA_1 + (1-d)A_2$

$BU = dB_1U_1 + (1-d)B_2U_2$, then

$$\begin{bmatrix} \frac{di_l}{dt} \\ \frac{di_1}{dt} \\ \frac{dv_c}{dt} \end{bmatrix} = \begin{bmatrix} -\frac{(R_c+R_l)}{L} & 0 & \frac{1}{L} \\ 0 & -\frac{R_a}{L_a} & 0 \\ -\frac{1}{C} & 0 & 0 \end{bmatrix} \begin{bmatrix} i_l \\ i_1 \\ v_c \end{bmatrix}$$

Where $A_1 = \begin{bmatrix} -\frac{(R_c+R_l)}{L} & 0 & \frac{1}{L} \\ 0 & -\frac{R_a}{L_a} & 0 \\ -\frac{1}{C} & 0 & 0 \end{bmatrix}$

And $B_1U_1 = \begin{bmatrix} 0 \\ 0 \\ 0 \end{bmatrix}$ (4)

Similarly when switch-1 is off mode and the switch-2 is conducting mode, the equations can be written based on KCL and KVL as:

$$C\frac{dv_c}{dt} = i_c = i_l - i_1 \quad (5)$$

$$L_a\frac{di_1}{dt}+R_a i_1+L\frac{di_l}{dt}+R_l i_l=v_c+(i_l-i_1)R_c \quad (6)$$

$$L\frac{di_l}{dt}=V_g-v_c-i_l(R_l+R_c)+i_1R_c \quad (7)$$

Simplifying eq. (6) and eq. (7), we get

$$\frac{di_1}{dt}=\frac{2v_c-V_g+2i_lR_c-2i_1R_c-i_1R_a}{L_a} \quad (8)$$

The state-space form of above equations can be represented as:

$$\begin{bmatrix}\frac{di_l}{dt}\\ \frac{di_1}{dt}\\ \frac{dv_c}{dt}\end{bmatrix}=\begin{bmatrix}-\frac{(R_c+R_l)}{L} & \frac{R_c}{L} & -\frac{1}{L}\\ \frac{2R_c}{L_a} & -\frac{(2R_c+R_a)}{L_a} & \frac{2}{L_a}\\ \frac{1}{C} & -\frac{1}{C} & 0\end{bmatrix}\begin{bmatrix}i_l\\ i_1\\ v_c\end{bmatrix}+\begin{bmatrix}\frac{V_g}{L}\\ -\frac{V_g}{L_a}\\ 0\end{bmatrix}$$

As we know, $A=dA_1+(1-d)A_2$ and $BU=dB_1U_1+(1-d)B_2U_2$

$$\text{Where } A_2=\begin{bmatrix}-\frac{(R_c+R_l)}{L} & \frac{R_c}{L} & -\frac{1}{L}\\ \frac{2R_c}{L_a} & -\frac{(2R_c+R_a)}{L_a} & \frac{2}{L_a}\\ \frac{1}{C} & -\frac{1}{C} & 0\end{bmatrix}$$

$$\text{and } B_2U_2=\begin{bmatrix}\frac{V_g}{L}\\ -\frac{V_g}{L_a}\\ 0\end{bmatrix} \quad (9)$$

Let the switching function of self commutated controlled switch-1 and switch-2 is q_1 and q_2 respectively. Assuming the continuous conduction mode, the averaged model is obtained by substituting d for q1 and 1-d(d') for q2.The state space average model is represented as mentioned previously:

$$\dot{X}=AX+BU$$

$$Y=CX$$

$$\text{Where } A=dA_1+(1-d)A_2 \text{ and}$$

$$BU=dB_1U_1+(1-d)B_2U_2 \quad (10)$$

Substituting eq.(4) and eq.(9) in eq.(10), that results:

$$A=\begin{bmatrix}-\frac{(R_c+R_l)}{L} & \frac{R_cd'}{L} & -\frac{(d'-d)}{L}\\ \frac{2R_cd'}{L_a} & -\frac{(2R_cd'+R_a)}{L_a} & \frac{2d'}{L_a}\\ \frac{(d'-d)}{C} & -\frac{d'}{C} & 0\end{bmatrix} \text{ And}$$

$$BU=\begin{bmatrix}\frac{V_gd'}{L}\\ -\frac{V_gd'}{L_a}\\ 0\end{bmatrix} \quad (11)$$

Hence the state-space average form for whole period can be written as:

$$\begin{bmatrix}\frac{di_l}{dt}\\ \frac{di_1}{dt}\\ \frac{dv_c}{dt}\end{bmatrix}=\begin{bmatrix}-\frac{(R_c+R_l)}{L} & \frac{R_cd'}{L} & -\frac{(d'-d)}{L}\\ \frac{2R_cd'}{L_a} & -\frac{(2R_cd'+R_a)}{L_a} & \frac{2d'}{L_a}\\ \frac{(d'-d)}{C} & -\frac{d'}{C} & 0\end{bmatrix}\begin{bmatrix}i_l\\ i_1\\ v_c\end{bmatrix}+\begin{bmatrix}\frac{V_gd'}{L}\\ -\frac{V_gd'}{L_a}\\ 0\end{bmatrix} \quad (12)$$

$$\begin{bmatrix}i_l\\ i_1\\ v_c\end{bmatrix}=\begin{bmatrix}1 & 0 & 0\\ 0 & 1 & 0\\ 0 & 0 & 1\end{bmatrix}\begin{bmatrix}i_l\\ i_1\\ v_c\end{bmatrix} \quad (13)$$

3 Small Signal Analysis

The state-space averaged model of Z-source converter with R-L load shown in (12) has non linear in nature as the control parameter (d) is in matrix A. Therefore small signal analysis is required to make the state-space to be linear. Due to small variation of $\hat{d}$ in steady state D the state variables are changed to $I_l + \hat{i}_l$, $I_1 + \hat{i}_1$, $and\ V_c + \hat{v}_c$.The state-space averaged model (12) and (13) with small perturbation is modified as:

$$\begin{bmatrix} \frac{d(I_l+\hat{i}_l)}{dt} \\ \frac{d(I_1+\hat{i}_1)}{dt} \\ \frac{d(V_c+\hat{v}_c)}{dt} \end{bmatrix} = \begin{bmatrix} -\frac{(R_c+R_l)}{L} & \frac{R_c(D'-\hat{d})}{L} & \frac{(D-D'+2\hat{d})}{L} \\ \frac{2R_c(D'-\hat{d})}{L_a} & -\frac{(2R_c(D'-\hat{d})+R_a)}{L_a} & \frac{2(D'-\hat{d})}{L_a} \\ \frac{-(D-D'+2\hat{d})}{C} & -\frac{(D'-\hat{d})}{C} & 0 \end{bmatrix}$$

$$\begin{bmatrix} I_l+\hat{i}_l \\ I_1+\hat{i}_1 \\ V_c+\hat{v}_c \end{bmatrix} + \begin{bmatrix} \frac{V_g}{L}(D'-\hat{d}) \\ \frac{-V_g}{L_a}(D'-\hat{d}) \\ 0 \end{bmatrix} \qquad (14)$$

$$\begin{bmatrix} I_l+\hat{i}_l \\ I_1+\hat{i}_1 \\ V_c+\hat{v}_c \end{bmatrix} = \begin{bmatrix} 1 & 0 & 0 \\ 0 & 1 & 0 \\ 0 & 0 & 1 \end{bmatrix} \begin{bmatrix} I_l+\hat{i}_l \\ I_1+\hat{i}_1 \\ V_c+\hat{v}_c \end{bmatrix} \qquad (15)$$

Subtracting steady-state representation of (12) from (14) and (13) from (15) neglecting higher order perturbation terms, the small signal model is:

$$\begin{bmatrix} \frac{d\hat{i}_l}{dt} \\ \frac{d\hat{i}_1}{dt} \\ \frac{d\hat{v}_c}{dt} \end{bmatrix} = \begin{bmatrix} -\frac{(R_c+R_l)}{L} & \frac{R_c(1-D)}{L} & -\frac{(1-2D)}{L} \\ \frac{2R_c(1-D)}{L_a} & -\frac{(2R_c(1-D)+R_a)}{L_a} & \frac{2(1-D)}{L_a} \\ \frac{(1-2D)}{C} & -\frac{(1-D)}{C} & 0 \end{bmatrix} \begin{bmatrix} \hat{i}_l \\ \hat{i}_1 \\ \hat{v}_c \end{bmatrix} + \begin{bmatrix} \frac{2V_c-V_g-R_cI_1}{L} \\ \frac{V_g-2V_c+2R_cI_1-2R_cI_l}{L_a} \\ \frac{(I_1-2\,I_l)}{C} \end{bmatrix} [\hat{d}] \qquad (16)$$

$$\begin{bmatrix} \hat{i}_l \\ \hat{i}_1 \\ \hat{v}_c \end{bmatrix} = \begin{bmatrix} 1 & 0 & 0 \\ 0 & 1 & 0 \\ 0 & 0 & 1 \end{bmatrix} \begin{bmatrix} \hat{i}_l \\ \hat{i}_1 \\ \hat{v}_c \end{bmatrix} \qquad (17)$$

4 Steady State Analysis and Design Consideration

The steady state equations can be derived from averaged state-space model (12) by simplification and represented as:

$$I_l = \frac{(1-D)I_1}{(1-2D)} \qquad (18)$$

$$V_c = \frac{(A+B)(1-D)(1-2D)\,V_g}{2A(1-D)(1-2D)+B(1-2D)^2} \qquad (19)$$

Where $A = 2D^2R_c - 2DR_c - R_l + DR_l$

$$B = 6D^2R_c - 10DR_c - R_a + 2DR_a$$

Under ideal condition (assuming ESR of inductance and capacitance is zero) then A=0; $B=R_a$ (2D-1), which gives:

$$V_c = \frac{(1-D)V_g}{(1-2D)} = I_1R_a \qquad (20)$$

Selections of passive parameters of X shaped network are based on minimization of current ripples and voltage ripples. It is also shown that the change of passive parameters affect the transient responses. It is therefore important to carefully select the Z-source L and C values to achieve a good compromise between oscillatory response, ripple factor and non minimum phase effect. Initially selection is based on ripple factor. A battery of 12V input is used in Z-source chopper to control the voltage across the load resistor. Let us assume that the voltage across the load of R (10Ω) is increased to 5 times (60V).The load current isI_1=6A. At rated voltage operation the voltage gain of Z-source chopper is found to be± 5 (60/12) and hence D is calculated from (20) under ideal condition and found to be D=0.445 for 60V and .545 for 60V with $I_l = \pm 6$A. Let the current ripple of $I_l$and the capacitor voltage ripples (v_c) are assumed to be

maximum limit of $\pm 1\%$, then $\Delta I_l = .06A$ and $\Delta v_c = 1.2$V. Assuming the operation of switch with switching frequency of 10KHz under full rated voltage condition, when the switch 2 is on for a period of (1-D)T second, then the inductor is calculated as: $L\frac{d\,I_l}{dt} = 12$ -(-60) and $L = \frac{72 * .0001 * .45}{0.06}$ then L =5.4mH, Hence choose $L = 6$mH. Similarly the value C is calculated by considering the switch1 in off condition using the equation (3), which gives C=1.375mF (approximately).

The ESR of capacitor depends on switching frequency and capacitance value of capacitor. The mathematical expression of ESR of capacitor is:

$$R_c = \frac{1}{\omega^2 {}_{R_{leak}} C^2}$$

The ESR effect of capacitor is negligible if the switching frequency is very high. The ESR of inductance depends on number of turns, diameter of wire and also switching frequency. The ESR of inductance increases with increase in frequency. The ESR sensitivity effect is shown in Fig 2.The boost capability decreases with increase the ESR value of capacitance and also inductance. The ESR value of inductance is more dominant to decreases the boost capability of Z-source converter compared to ESR value of capacitor. From the figures, it is also found that the Z-source chopper posses boost capability with same polarity as input in the duty ratio range between 0<D<0.5 and both boost and buck capability with reverse polarity in the duty ratio range between 0.5<D<1.

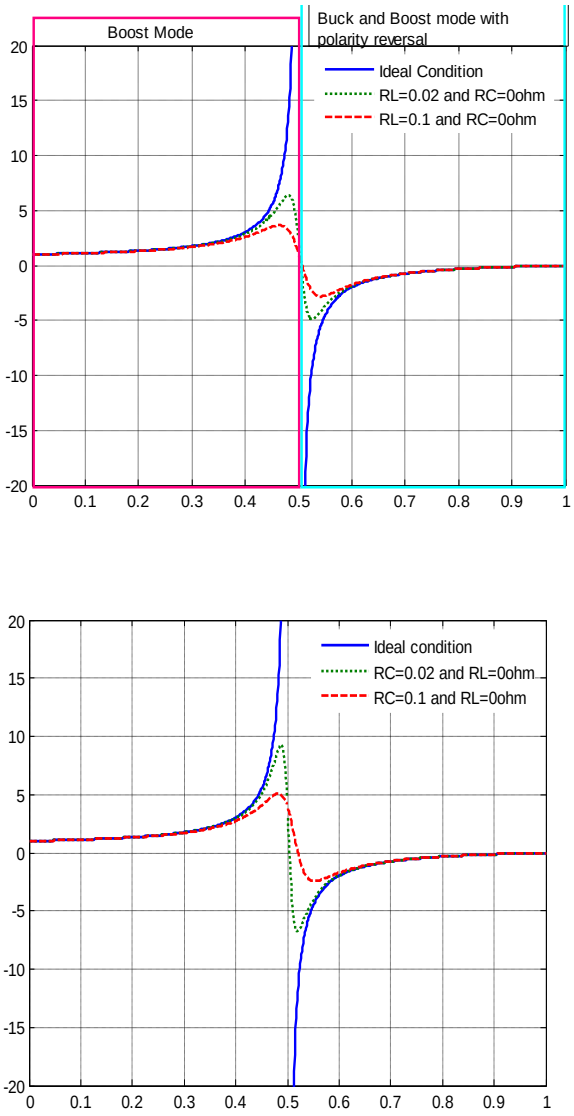

Fig 2 (a, b): Voltage gain versus duty cycle of Z-source chopper with and without ESR of inductance and Capacitance.

The transfer functions (21), (22) and (23) are derived from small signal model given in (16) and (17) at D=0.4 using the parameters as given in Table 1.here in table 1 the parameters are justified from the Simulink model.

Table 1

V_g	R_a	RL (ESR)	L	L_a	C	RC (ESR)
12V	10 Ω	0.02 Ω	4 mH	2 mH	1.375 mF	0.12 Ω

$$Gild(S) = \frac{\hat{i}_l(S)}{\hat{d}} = \frac{1.26*10^4 S^2 + 6.42*10^7 S + 5.52*10^9}{S^3 + 5.1*10^8 S^2 + 4.45*10^5 S + 4.29*10^7} \quad (21)$$

$$Gi1d(S) = \frac{\hat{i}_1(S)}{\hat{d}} = \frac{-2.62*10^4 S^2 - 6.88*10^6 S + 7.14*10^8}{S^3 + 5.1*10^8 S^2 + 4.45*10^5 S + 4.29*10^7} \quad (22)$$

$$Gvcd(S) = \frac{\hat{v}_c(S)}{\hat{d}} = \frac{-1.14*10^4 S^2 - 4.52*10^7 S + 7.25*10^9}{S^3 + 5.1*10^8 S^2 + 4.45*10^5 S + 4.29*10^7} \quad (23)$$

Where $Gild(S), Gi1d(S)$ and $Gvcd(S)$ is denoted as control-to-inductor current, control-to-load current, control-to-capacitor voltage transfer functions respectively.

5 Transient Analysis

Before attempting the closed loop control of Z-source chopper it is necessary to study the transient behaviour which depends on passive parameters and its ESR value. To date, many methods for modeling of power converters have been reported in the literature[6]-[9].Here commonly adopted average state space analysis with small signal method is used to study the transient behaviour of open loop system with step changes of duty cycle.

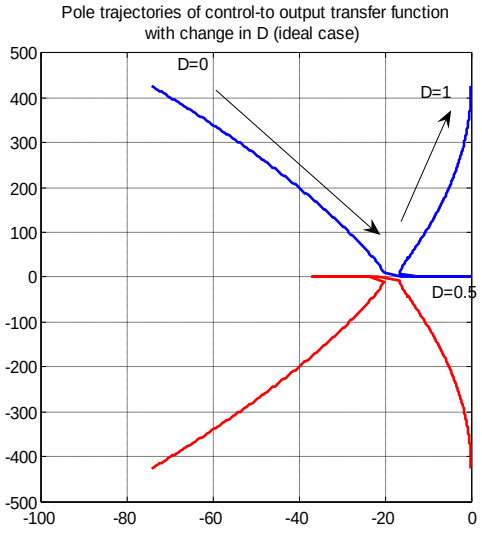

Fig 3 (a, b): Pole trajectories of Z-source chopper with and without ESR Capacitance.

To control the wide range of output voltage, it is important to study the movements of poles and zero in order to maintain acceptable performance and stability[10]-[15]. Fig 3(a, b) shows the poles trajectories of control-to output transfer function with change in D from 0 to 1 with and without the ESR value. Under ideal case (without ESR) the one of the pole is lying on the real axis and is far away from the imaginary axis and therefore the effect of this pole is negligible in transient response. Therefore under ideal condition the system analysis can be easily controlled by considering the system as a second order system [16], [17]. The effect of ESR is shown in the figure. The one of the pole which is far away from the imaginary axis under ideal case is moving towards the imaginary axis and the movement speed depends upon the value of ESR. The other two poles moves slightly away from the imaginary axis. All the three poles are the dominant poles and have impact on the transient response particularly in the range of D from 0.4 to 0.7. The movement of poles away from imaginary axis and one pole which is far away from the imaginary axis moves towards the imaginary axis due to ESR improves the transient response. The overshoot and undershoot are reduced, which reduces the system damping and also settling time. Thus with ESR the transient responses are improved but the boost capability of system is greatly reduced with increase in ripples and incurred more loss in system. The above conclusions are observed by simulating the Z-source chopper by step changing the D from 0.3 to 0.4 and 0.7 to 0.6.The simulated

responses of control-to-capacitor voltage, control-to-inductor current and control-to-load current during step change in D from 0.3 to 0.4 and 0.7 to 0.6 are shown in Fig.(5) and Fig.(6) respectively.

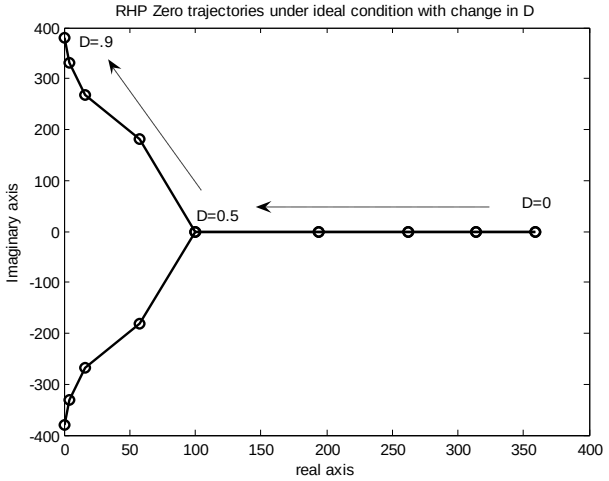

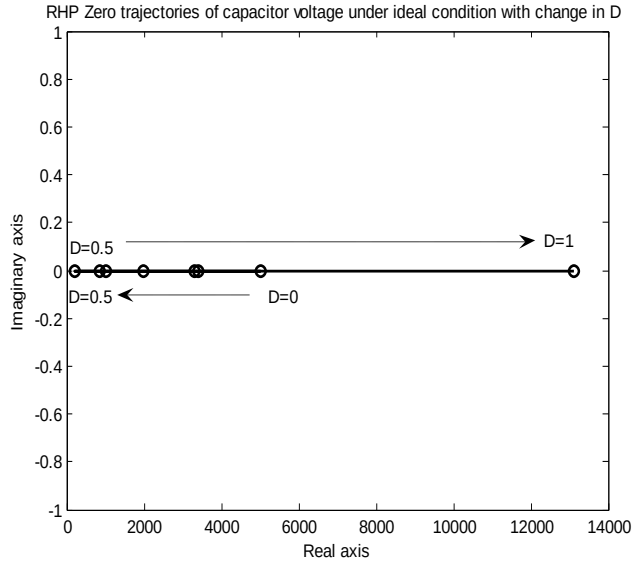

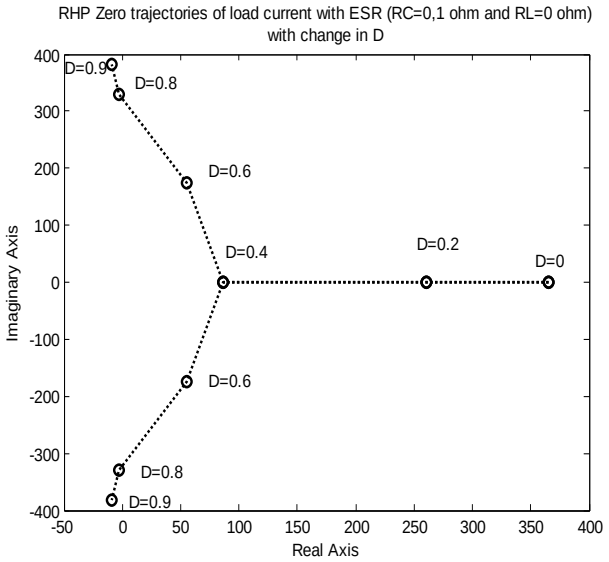

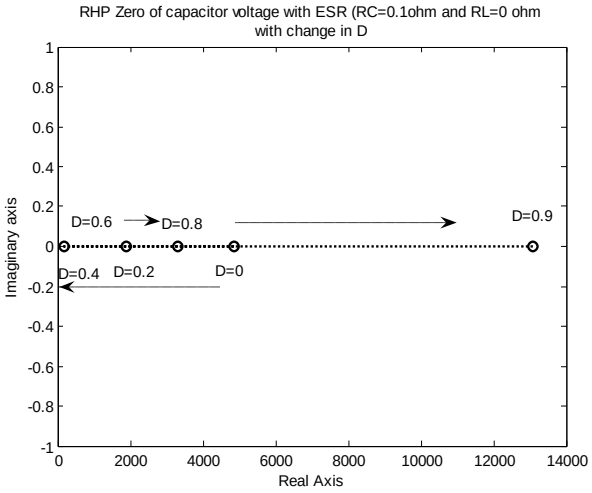

Fig 4 (a, b, c, d): RHP Zero trajectories of Z-source chopper of load current and capacitor voltage with and without ESR.

It is necessary to study the non-minimum phase effect of control-to-output transfer functions with and without ESR to analysis the dip caused during sudden change in the step command. As shown in Fig.(4),the control-to-load current and control-to-capacitor voltage transfer functions posses the non-minimum-phase transient because of presence of zero in right side of S plane (RHP zero) whereas control -to- inductor current transfer function has non-minimum-phase transient. Due to non-minimum phase effect of control-to-inductor current transfer function, the dip in transient response is zero at the instant of step increase in D and it is confirmed by Fig.5 (b).The dip will be created in control-to-load current and control-to-capacitor voltage transfer functions at the instant of step increase in D because of the presence of Zero in right side of S plane. The RHP zero movement of control-to-load current and control-to-capacitor voltage transfer functions due to change in D with and without ESR are shown in Fig(4).The movement of RHP zero towards imaginary axis is faster with increase of ESR value as compared to ideal condition (without ESR) especially, in the range of D from 0.3 to 0.6. Therefore The increase of ESR value of X network of Z-source chopper increases the non- minimum-phase undershoot (created large dip at the instant of change in D) . For illustrating the non–minimum-phase undershoot of the different transfer functions of Z-source chopper, an initial condition of D=0.3 and 0.7 are assumed. With step change of D from 0.3 to 0.4 at .4 second and 0.7 to 0.6 at 1second, the simulations are carried out in Matlab/simulink environment by taking MOSFET as controlled switch.Fig.5(a,b,c) and Fig.6(a,b,c,) show the step responses of control-to-

capacitor voltage, control-to-inductor current and control-to-load current respectively with and without ESR. The figure of control-to-capacitor voltage, control-to-load current clearly shows that there is a large dip of load current and capacitor voltage as compared to ideal condition at the instant of transient before rising the towards their new steady-state values non-minimum-phase features for RHP zero. It is proved by other researcher that the increase of inductance of X network of Z-source parameters increases the system damping with a reduced overshoot and undershoot but an increased rise time and settling time due to shifting of dominant poles toward the origin of complex plane[7]. The increase of inductance of X network of Z-source parameters increases the non-minimum-phase undershoot due to shifting of RHP zero toward the origin of complex plane, whereas the increase of capacitance has negligible effect on non-minimum-phase undershoot of load current and capacitor voltage[7].

It is therefore concluded that the Shifting of RHP zero towards imaginary axis due to ESR value increases non-minimum-phase undershoot, whereas movement of one of the poles towards imaginary axis decreases the system settling time and oscillatory response. Further with increase of ESR value decreases the boost capability of Z-source chopper and introduce large ripple in output signal. For a more effective implementation of feedback control for boosting operation of Z-source chopper for voltage control, it is recommended that instead of armature current feedback ,the inductor current feedback can be used, which eliminate the non-minimum-phase effect. In this paper the compensators design are explained in next subsection by taking the inductor current feedback.

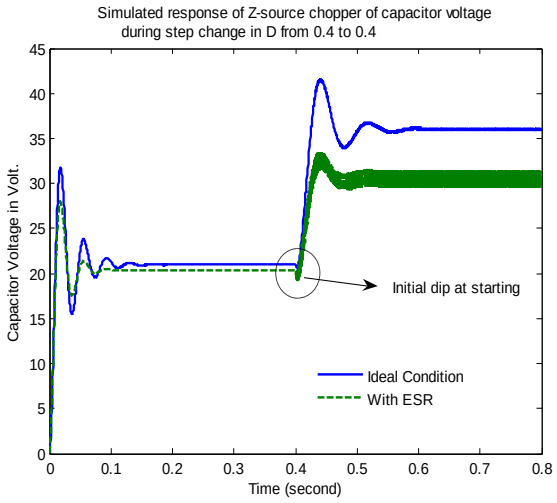

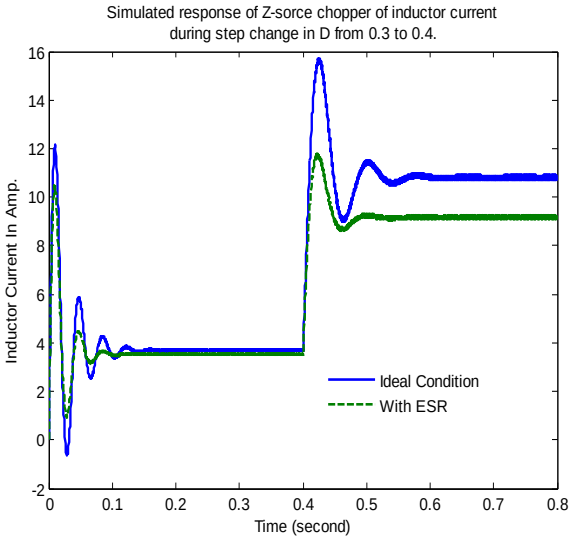

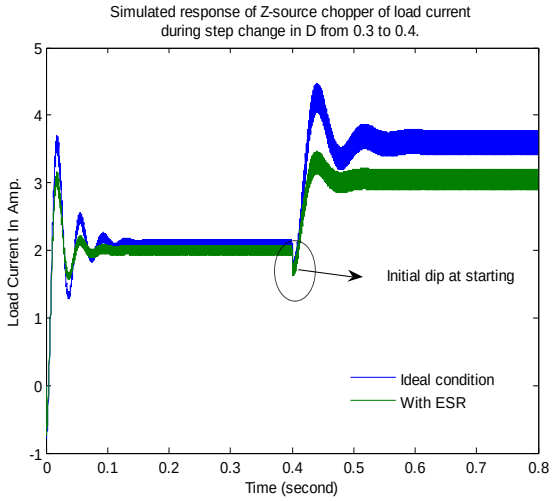

Fig 5 (a, b, c): Simulated response of Z-source capacitor voltage, inductor current and load current during a step change in D from 0.3 to 0.4 respectively.

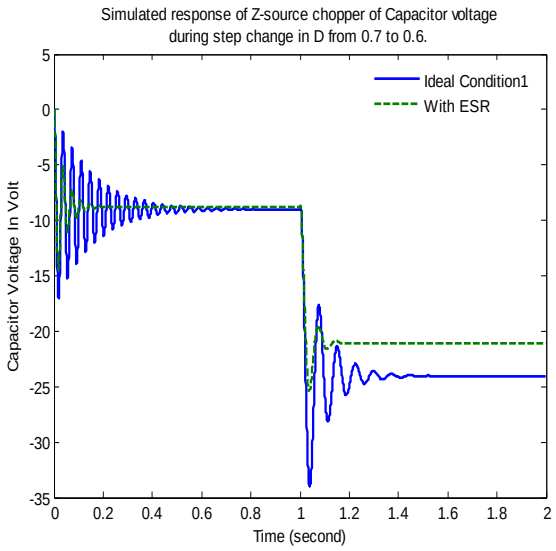

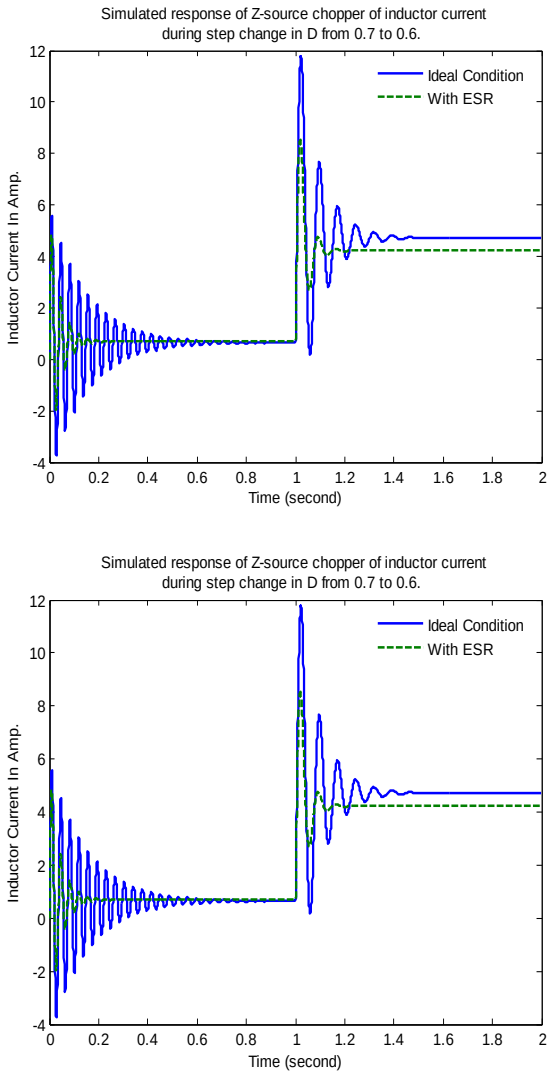

Fig 6 (a, b, c): Simulated response of Z-source capacitor voltage, inductor current and load current during a step change in D from 0.7to 0.6 respectively.

6 Current Mode Control of Z-Source Chopper

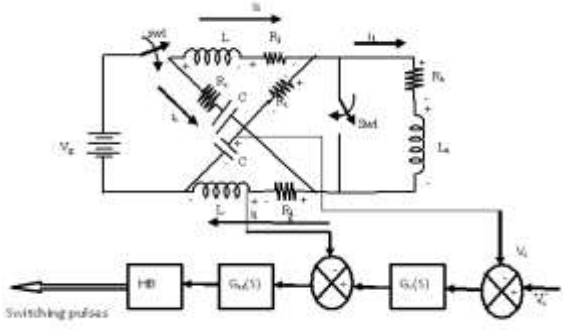

Fig 7: Circuit diagram of Z-source chopper with feedback control circuit

The derived transfer functions from small signal model can be used for current mode control method. In current mode control method there are two loops one is inner input current loop and other is outer capacitor voltage loop where actual voltage follow the reference voltage. In inner loop, the direct measurement of inductor current is compared with the reference inductor current estimated from the outer loop.

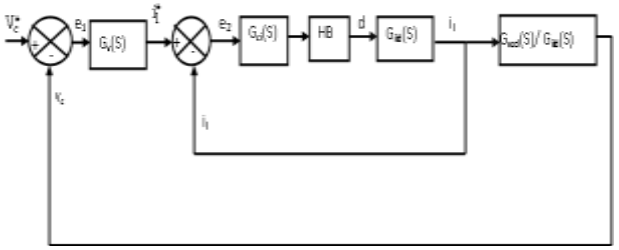

Fig 8 : Block diagram of closed loop capacitor voltage control.

The error is compensated using $\mathrm{Gci(S)}$.Hence the loop transfer function of inner current loop is $\mathrm{Gci(S)} * \mathrm{Gi1d(S)}$.The switching function $\hat{d}$ is determined from the output of $\mathrm{Gci(S)}$ through hysteresis band controller.In outer voltage loop, the direct measurement of capacitor voltage is compared with reference voltage. The error is compensated using $\mathrm{Gv(S)}$.The output of $\mathrm{Gv(S)}$ is the inductor input current command which is processed by actual current by inner loop. The block diagram of current control mode is shown in Fig 8. The outer loop is highly coupled with inner loop because of inductor current command is generated from outer loop which is the command value of inner loop [4]. The coupling behavior can be represented by transfer function is as follows:

$$(\hat{\imath}_l^* - \hat{\imath}_l)\mathrm{Gci(S)} = \hat{d} \qquad (24)$$

Substituting the value of $\hat{\imath}_{l1}$ in eq.(24):

$$\hat{\imath}_l^* * \mathrm{Gci(S)} = \hat{d}(1 + \mathrm{Gild(S)Gci(S)}) \qquad (25)$$

Solving eq.(25) and eq.(23) then inductor current command-to-speed transfer function will be

$$Gvil(S) = \frac{\hat{v}_c(S)}{\hat{i}_1^*(S)} = \frac{Gvcd(S)*Gci(S)}{(1+Gild(S)Gci(S))} \quad (26)$$

7 Compensator Design

Based on the small signal expressions of the Z-source chopper the compensators blocks $Gci(S)$ and $Gv(S)$ are designed using the design specifications given in Table-1without ESR. First, the inner current loop compensator is designed based on frequency response. The bode plot of $Gild(S)$ at D=.3 and .4 is given in Fig.9 (a,b) It can be observed that the three closed loop poles are on the negative side of real axis of the complex plane. One of the closed loop pole is very close to imaginary axis (-80) and other two poles are far away from the imaginary axis ($-1.5*10^4$,$-5*10^3$). The phase margin of open loop transfer function at D=0.4 is 90^0 at gain cross over frequency $1.5*10^4$ rad/s. It is also observed that the closed loop pole which is near to the imaginary axis moves towards the imaginary axis with increase in D up to 0.5 whereas the far away poles moves away from the imaginary axis, which increases the gain cross over frequency($7.5*10^3$ at D=0.3 to $1.5*10^4$ at D=0.4). Since gain cross over frequency increases with increase in D from 0 to 0.5 the band width is increased, which causes high picking behaviours to noise. In order to reduce the high picking behaviours and band width, the PI compensator is used in inner loop which act as low pass filter. The root locus technique is used for design of compensator to place the closed loop poles in order to get best performances. From root locus diagram the inner compensator is designed and found to be

$$Gci(S) = 2.5\frac{(1+0.25S)}{S} \quad (27)$$

The compensated bode diagram and root locus of inner loop transfer function is shown in Fig.10.In this design the gain crossover frequency is decreased from $7.5*10^3$ rad/sec to $4.5*10^3$. It is important to note that the inner loop must be must faster than the outer loop to prevent any clashes between the two loops [5]. In outer speed control loop, the PI compensator is used to meet the capacitor voltage to command duty ratio (d) value with good transient response. Although it is difficult to get desired transient performances such as increase of speed behaviours, decrease of overshoot and settling time by using any of the classical compensators, because of all the poles are not available for placing at desired location, but the gains of fixed compensator are determined in such a way that the non dominant poles are placed far away from the dominant poles to reduce the transient effects created by dominant poles. Here the uncompensated system is unstable because one of the closed loop pole is closed to origin but in right side of S-plane. Hence lead compensator is used to improve transient response and make it stable by moving the unstable pole towards left half of S-plane. The drawback of lead compensator increases the steady state error. The gains of lead compensator are selected based upon the trade-off between transient response and steady-state error. The selection of gains of compensator is carried out by root-locus method and it is verified by bode diagram using Control toolbox in MATLAB environment.

The bode diagram of uncompensated and compensated loop transfer functions of speed loop are shown in Fig.11and Fig.12 respectively. The compensator for capacitor voltage loop used for control of output voltage derived from root locus tool box is expressed as:

$$Gv(S) = \frac{(S+4)}{(S+20)} \quad (28)$$

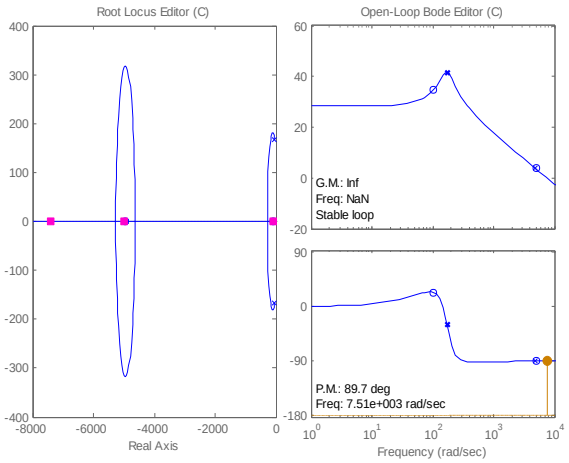

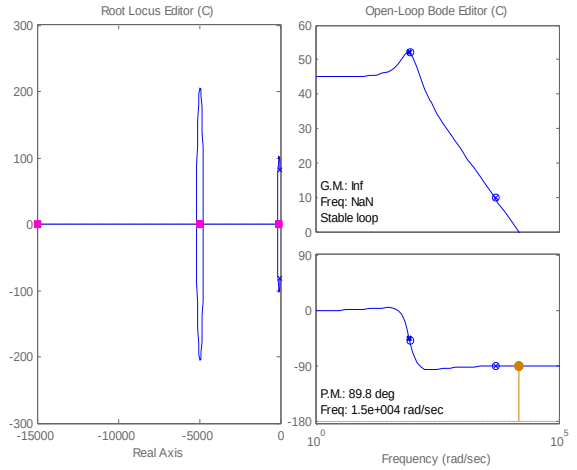

Fig 9 (a, b): Root locus and Bode plot of uncompensated $Gi1d(S)$ for CM control (Fig.9(a) for D=0.3 and Fig.9(b) for D=0.4).

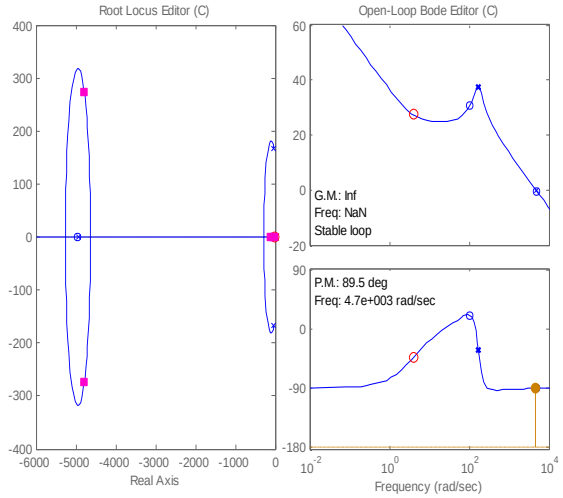

Fig 10: Root locus and Bode plot of compensated $Gi1d(S)$ for CM control.

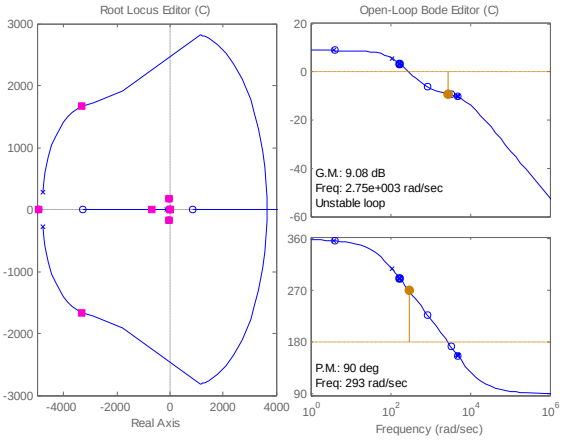

Fig 11: Root locus and Bode plot of uncompensated $Gvil(S)$ for capacitor voltage control

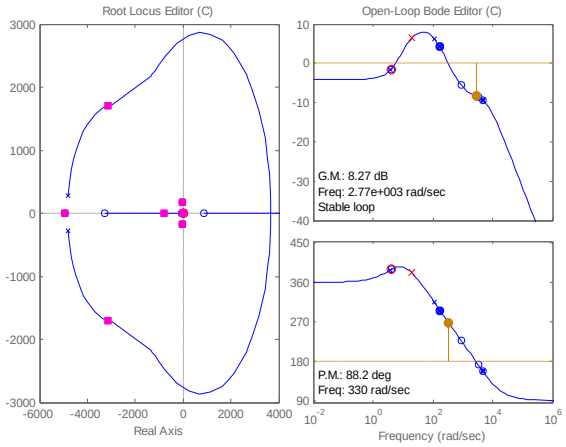

Fig 12: Root locus and Bode plot of compensated $Gvil(S)$ for capacitor voltage control

8 Simulation Results

In order to verify the proposed control strategy of current mode control technique used for capacitor voltage control, simulations are carried out using Matlab/Simulink software. The same circuit parameters are used as in Table-1 without ESR. The designed compensators gain using (27) and (28) are used for inner loop and outer loop respectively. Step responses of 36V for 2 second and at 2 second step response command increased to 60V are used to observe the dynamic characteristics of capacitor voltage, inductor current, and load current respectively. Fig 13 (a,b,c) shows the capacitor voltage, inductor current, and load current responses of change of step reference from 36 V to 60V respectively. It has been observed that both of the speed responses reach the respective steady state value without exhibiting the oscillation. The settling time for high capacitor voltage response is higher than the low capacitor voltage step response command. It can be observed from Fig-13(a) that there is no dip in voltage response at the time of starting of transient due to sudden change of command speed from 36V to 60 V. Settling time for 36V is 0.5 second and for 60V it is about 0.9 second. The ripple of load current, which depends upon hysteresis band controller and inductance of the circuit, is found to be $\pm 1\%$ with average steady value 3.5Ampere for low voltage step command of 36V and average steady state value of 6Ampere for high Voltage reference of 60V.

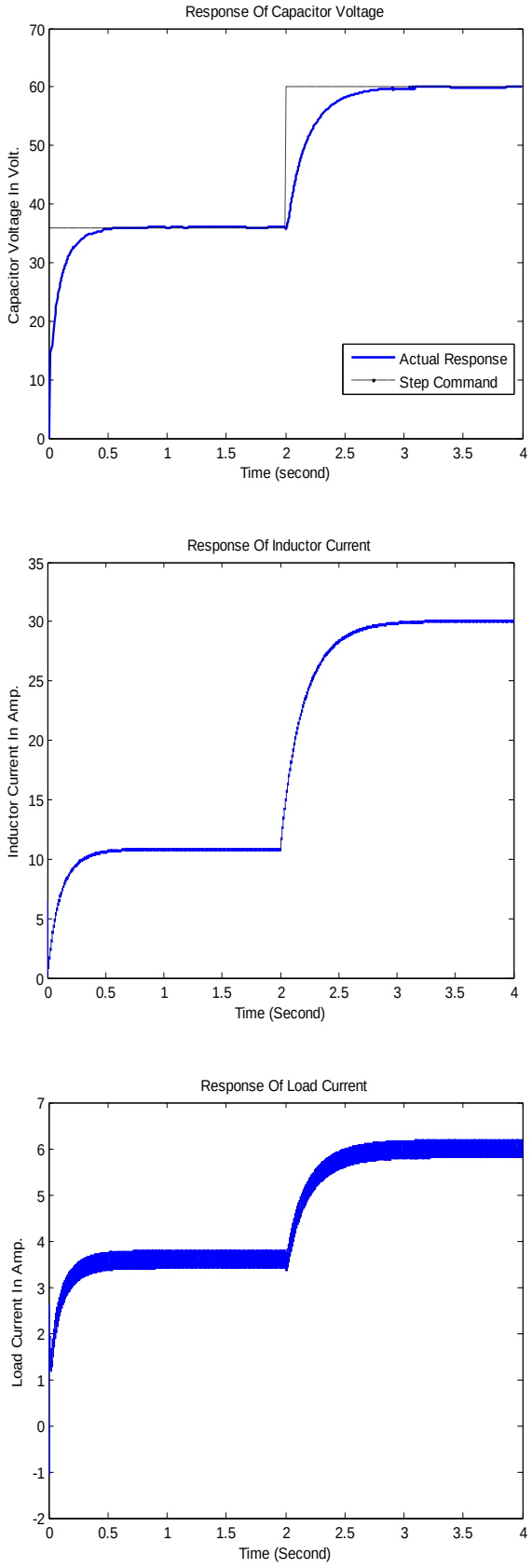

Fig 13(a, b, c): Capacitor voltage, Inductor Current , Load Current responses of closed loop Z-source chopper control of R-L load for a change of step response from 36 V to 60 V.

9 Conclusion

This paper presents detailed transient analysis on Z-source chopper with ESR effect used for capacitor voltage control under R-L load using small signal model. The study of transfer function of control -to-output has revealed that the existence of RHP zero which depend on ESR value of passive parameters and control parameter mainly on load current and capacitor voltage causes dip in output responses due to sudden change of capacitor voltage command. However, the dip in inductor current is zero because of non existence of RHP zero as a result; the inner feedback inductor current control is used to study the closed loop capacitor voltage control instead of load current feedback. The compensators for the capacitor voltage loop and the current loop are designed based on the frequency responses and as well as root locus technique. The oscillation and slower rise time can be improved by suitable design of compensator and using hysteresis band controller. The simulation responses of capacitor voltage, load current and inductor current for boosting of voltage are presented by suitable design of compensators.

References:

[1] F.Z.Peng, Z source inverter, *IEEE Transactions on Industrial Application*, Vol.39, No.2, 2003, pp.504-510.

[2] B.K.Nayak, Saswati Swapna Dash, Performance Analysis of Different Control Strategies in Z-source Inverter, *ETASR-Engineering, Technology & Applied Science Research*, Vol.3, No.2, 2013, pp.391-395.

[3] J.Liu, J.Hu, and L.Xu, Dynamic Modeling and Analysis of Z Source Converter Derivation of AC Small Signal Model and Design-Oriented Analysis, *IEEE Transactions on Power Electronics*, Vol.22, No.5, 2007, pp 1786-1796.

[4] F.Z.Peng, M.Shen, and Z.Quin, Maximum boost control of Z-source inverter, *IEEE Transactions on Power Electronics*, Vol.20, No.4, 2005, pp 883-838.

[5] Gokhan Sen and Malik Elbuluk,Voltage and Current Programmed Modes in control of the Z-Source Converter, *IEEE Transactions on Industry Applications*, Vol-46, No. 2, 2010, pp.680-686.

[6] C.J.Gajanayake, D.Mahinda and Poh.Chiang Loh, Small-Signal and Signal-Flow-Graph Modeling of Switched Z-source Impedance Network, *IEEE Power Electronics Letter*, Vol.3, No.3 2005.

[7] Poh.Chiang Loh, D.M.Vilathgamuwa, C.J.Gajanayake and C.W.Teo, Transient

Modeling and Analysis of Pulse-width_modulated Z-Source Inverter, *IEEE Transactions on Power Electronics*, Vol.22, No.2, 2007, pp.498-507.

[8] F.Z.Peng, X.M.Yuan, X.P.Fang, and Z.M.Quin, Z source inverter for adjustable speed drives, *IEEE Power Electronics Letter*, Vol.1, No.2, 2003, pp.33-35.

[9] K.Smedley,and S.Cuk, Switching flow graph nonlinear modelling technique, *IEEE Transactions on Power Electronics*, Vol.9, No.4, 1994, pp.405-413.

[10] R.D.Middlebrook and S.Cuk, A general unified approach to modelling switching converter power stages, *IEEE PESC proceedings*, 1976,pp.18-34.

[11] P.T.Krein, *Elements of Power Electronics*, New York:Oxford University Press,1998.

[12] G.F.Franklin, J.D.Powel and A.Emami-Naeini, *Feedback Control of Dynamic Systems*, MA:Addison-Wesley,1994.

[13] R. Aaron Kelvin, Noreen L. Foster, Dannielle P. Hazel and A. M. Hasanul Basher, Closed-loop position control system using labview, *Southeast conference*, 2002, pp.283-286.

[14] R.Krishnan, *Electric motor drives modeling, analysis and control*, Pearson education (singapore) pvt.ltd, 2003.

[15] L.Umanand, *Power electronic essentials and applications*, Wiley publishers, 2009.

[16] B.K. Nayak and S. S. Dash, Transient modeling of Z-source chopper used for adjustable speed control of DC motor drive, *IEEE Fifth Power India Conference*, 2012, pp. 1-6.

[17] B.K.Nayak, Saswati Swapna Dash, Battery Operated Closed Loop Speed Control of DC Separately Excited Motor by Boost-Buck Converter, *IEEE International conference on power electronics (IICPE-2012)*, 2012.